# Exploring the Evolution of Pressure-Perturbations to Understand Atmospheric Phenomena

Wathsala Widanagamaachchi[1*] Alexander Jacques[2†] Bei Wang[1*] Erik Crosman[2†]
Peer-Timo Bremer[1,3‡] Valerio Pascucci[1*] John Horel[2†]

[1]SCI Institute, University of Utah [2]Department of Atmospheric Sciences, University of Utah [3]Lawrence Livermore National Laboratory

**ABSTRACT**

Atmospheric sciences is the study of physical and chemical phenomena occurring within the Earth's atmosphere. The study entails understanding the state of the Earth's atmosphere, how it is changing over time and why. Understanding how various weather events develop and evolve is often conducted through retrospective analysis of past atmospheric events. Atmospheric scientists can then utilize tools to better predict potential hazards and provide earlier warnings for events that may impact life and property. Several atmospheric state variables can be measured to identify high-impact events, one of which is surface atmospheric pressure. Many weather events are characterized by variations in surface pressure from the mean pressure value (i.e., pressure-perturbations). Accordingly, there is significant interest in extracting and tracking pressure-perturbations both spatially and temporally to better understand the evolution of weather events.

Here, we present a visualization and analysis environment that allows interactive exploration of pressure-perturbation data sets. Our system, for the first time, enables atmospheric scientists to interactively explore the spatiotemporal behaviors of pressure-perturbations for a range of values and provides support to leverage other conventional data sets such as radar imagery and wind observations. It also allows atmospheric scientists to evaluate model and parameter sensitivity, which is difficult if not impossible with conventional visualization tools in atmospheric sciences. Finally, we demonstrate the utility of our approach for retrospective analysis using different case studies of recorded severe weather events.

**Index Terms:** E.1 [Data Structures]: Graphs and Networks—; J.2 [Physical Sciences and Engineering]: Earth and Atmospheric Sciences—

## 1 INTRODUCTION

Every day, a huge amount of data is collected with respect to surface atmospheric observations, such as temperature, pressure, moisture, and wind speed. There is a significant need to analyze and interpret these data to better understand the temporal evolution and the present state of the Earth's atmosphere from both research and operational (e.g., weather forecasting) perspectives. Atmospheric surface pressure is one of many measurements atmospheric scientists utilize, as it can be used to accurately characterize a wide variety of different weather systems. There are several benefits to using surface pressure over other atmospheric parameters. First, high-impact weather phenomena such as individual thunderstorms, hurricanes, and snowstorms all produce pressure-perturbations that vary in both magnitude and time. Second, pressure observations from non-conventional resources are less sensitive to nearby obstacles compared to other variables such as temperature (e.g., a temperature sensor located on the roof of a metal building) and wind (e.g., a wind sensor located in a region surrounded by trees). Third, surface pressure also provides information on the vertical structure of the atmosphere. For example, pressure-perturbations that occur above the surface may still be sensed by recording the pressure, as opposed to recording just temperature and wind speed. Fourth, pressure observations can be more readily assimilated into operational numerical weather prediction models with less concern for observation accuracy [15].

Therefore, it is beneficial to use surface pressure to characterize a wide variety of weather events. The ability to interactively extract, explore, and characterize pressure-perturbations both in space and across time to better understand atmospheric phenomena has the potential to greatly improve the understanding of past weather events as well as provide forecasters the ability to "nowcast" (i.e., a short-term forecast for 0-6 hrs) future events by assessing the pressure-perturbations with respect to other data sets such as radar imagery and wind observations on a single interactive interface.

Understanding these types of atmospheric phenomena requires identifying and extracting the feature-of-interest (i.e., *pressure-perturbation event*) within each time step of the data. Typically, a pressure-perturbation event is defined to be a single region in the domain where all the pressure-perturbation values are above/below a given threshold value. Often, such events are referred to as positive- or negative-pressure-perturbation events, respectively. Once features are extracted, they need to be correlated across adjacent time steps. Usually, feature correlations for atmospheric data are computed based on spatial overlap or distance proximity. Then, the resulting feature tracks (i.e., trajectories taken by individual features) are analyzed.

In this paper, we enable atmospheric scientists to extract pressure-perturbation events across multiple parameter values and explore their evolution with the aid of *tracking graphs* [25], where feature evolution is displayed as a collection of feature tracks, see Figure 1. Additionally, we provide scientists with a visualization and analysis environment to allow interactive exploration of pressure-perturbation data sets, see Figure 2. To better understand atmospheric phenomena, our system provides support to leverage other conventional data sets such as radar imagery and wind observations. Finally, in collaboration with atmospheric scientists, we apply our visualization and analysis environment to three case studies describing real world, high-impact atmospheric phenomena. Specifically, these case studies are extracted from pressure-perturbation data sets that

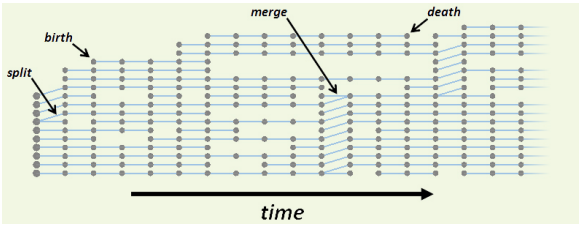


Figure 1: An example tracking graph showing the evolution of features across time. Within the graph, each set of nodes in a vertical column represents features in one time step and shows the "tracks" of each feature as it evolves: splitting, merging, or disappearing.

*e-mail: {wathsy, beiwang, pascucci}@sci.utah.edu
†e-mail: {alexander.jacques, erik.crosman, john.horel}@utah.edu
‡e-mail: bremer5@llnl.gov

2017 IEEE Pacific Visualization Symposium (PacificVis)
18-21 April, Seoul, Korea
978-1-5090-5738-2/17/$31.00 ©2017 IEEE

are generated by combining high-resolution grids of numerical simulations [20] with high-frequency pressure observations [19, 27]. For all case studies, with the help of our visualization environment, scientists are able to extract and explore the evolution of pressure-perturbation events to better understand their characteristics, as well as to evaluate their model and parameter sensitivity.

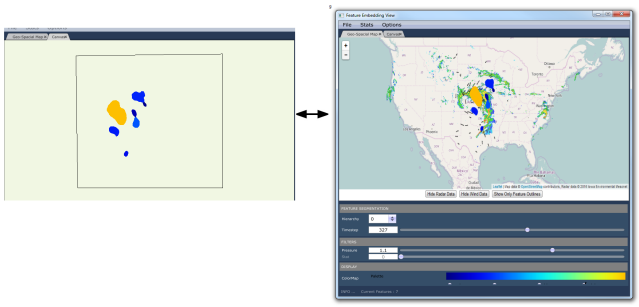

(a) Feature embedding view

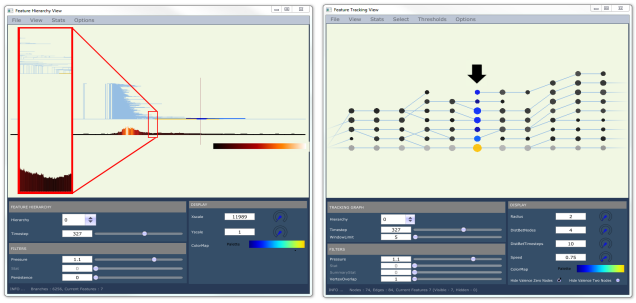

(b) Feature hierarchy view (c) Feature tracking view

Figure 2: Our framework contains three views, using data from case study III. (a) Shows the data embedding of features using two subcomponents: geometric embedding (left) and geospatial view (right). The geospatial view displays geographical information of features as well as various ancillary data such as radar and wind observations whereas the geometric embedding view displays the geometric information of the embedded features. (b) Visualizes the horizontal graph layout of the feature hierarchy along with a histogram-based view that summarizes the stability of features. Here, a zoomed-in view of the feature hierarchy (red box top) and histogram (red box bottom) is also displayed. Finally, (c) Shows the evolution of features using a tracking graph for a user-selected focused time step (indicated with a black arrow) and a time window.

## 2 Related Work

In this section, we present some relevant work to provide context and background for our research.

**Atmospheric Sciences.** Many prior studies analyze various atmospheric events associated with pressure-perturbations. These approaches attempt to analyze various atmospheric case studies with respect to such factors as types of atmospheric environment that lead to the formation of pressure-perturbation events [16]; comparisons across various atmospheric events [21]; and insights that can be gained from a specific pressure-perturbation event [13]. However, the ability to interactively visualize such events without drastic customization remains difficult. With our work, scientists have the flexibility to explore pressure-perturbation events and their evolution for the entire parameter space, which allows them to effectively analyze a wide range of atmospheric phenomena.

In a prior work, Jacques et al. [11] visualized and analyzed the frequency and amplitude of pressure-perturbations as a function of location and season at individual observing sites from the USArray Transportable Array (TA) surface station network (further described in Section 5). However, when visualizing pressure observations over time, they consider one single observing site at a time without considering other nearby stations that may be experiencing the same pressure-perturbation from the same weather phenomenon. Thus, spatial properties for the sensed pressure-perturbations were not initially assessed. Additional work has been conducted to assess spatial properties (e.g., size, magnitude, speed, and direction of movement) of prominent mesoscale features over extended monthly periods, but only by setting specific pressure-perturbation thresholds a priori [10]. In this work, we expand the work described in [10], and enable the atmospheric scientists to interactively vary the thresholds to understand parameter sensitivity, to evaluate feature extraction and movement without restrictive assumptions, and to leverage the extracted features with conventional data sets in a simple and concise manner.

**Feature Extraction and Tracking.** When analyzing time-varying data sets, feature extraction and tracking are usually employed to better understand their spatiotemporal behaviors. Among the many feature definitions existing in the literature, for the scope of this work, we are interested only in threshold-based features of a scalar field. Traditionally, isosurfaces [14] and interval volumes [6] are used to extract such threshold-based features. However, these approaches require repeated processing whenever a change is made for the parameter values. In contrast, techniques such as Morse-Smale complex [7], contour trees [4], and merge trees [3] extract features across a large range of threshold values in a single pass. Therefore, these approaches have gained more research interest in recent years.

Existing feature tracking techniques can be broadly classified into two categories: region-based and attribute-based correlations. With sufficient temporal resolution in the source data, region-based techniques determine the feature correlations by their spatial overlap [23], sometimes under affine transformations [12]. In attribute-based techniques, various feature-based attributes (e.g., centroid, mass, and volume) are used as a simplified model to characterize features and identify their correlations across time [22].

Our framework supports arbitrary feature definitions and correlation metrics. Specifically, we allow any of the standard clustering algorithms to define hierarchical features and any existing feature correlation criteria to define correlations. In the setting of atmospheric sciences, our collaborating scientists have very specific metrics in mind (i.e., spatial overlap and distance proximity-based metrics), and our framework is general enough to be successfully adapted to suit their needs.

**Time-varying Data Visualization.** Due to the dynamic behaviors within time-varying data sets and the large and diverse volumes of data available, visualizing time-varying data is considered to be a very challenging problem. Very different techniques have been developed depending on the subject area for understanding the evolution of time-varying features. Even so, they all focus on constructing effective data representations to convey the dynamic nature of these data. Illustration, abstraction, art, morphing, and animation are some of the traditional techniques for visualizing time-varying data sets [17]. Unfortunately, they often fail to scale to larger data sets and tend to be highly specialized to particular use cases. Tracking graphs [22, 25], where feature evolution is displayed as a collection of feature tracks, is considered to be a more effective method for visually summarizing feature evolution over time. As data become increasingly large and complex, tracking graphs can also become incomprehensibly large. However, various filtering, compression, and summarization techniques can be applied to produce high-level overviews. In this work, we combine tracking graphs with progressive filtering, simplification, and graph layouts to visualize the evolution of pressure-perturbation events.

## 3 Application Challenges

Surface pressure observations have been used to identify and track a variety of atmospheric systems. Many techniques have been utilized to help isolate atmospheric phenomena on time scales known in the discipline as synoptic (lasting 1-5 days), sub-synoptic (lasting several hours up to 1 day), and mesoscale (lasting minutes to several hours), as described in [11]. For the scope of this paper, we are predominantly concerned with events that are defined as mesoscale (lasting 10 mins to 12 hrs), although all techniques presented here can be applied to other timescales as well. High-impact atmospheric events at shorter scales, such as mesoscale convective systems that can contain severe thunderstorms, are often associated with large, quick (10 mins - 12 hrs) pressure-perturbations in the surface pressure field. It has been observed that gradients of these pressure-perturbations can result in strong, damaging winds. Consequently, although occurring fairly infrequently, these types of events have the capability to produce extensive property damage and can threaten human life. Therefore, understanding these short-term but high-impact events is of great value to atmospheric scientists. However, a number of practical challenges exist when analyzing pressure-perturbation data sets.

First, atmospheric scientists wish to explore pressure-perturbation events across multiple pressure-perturbation thresholds automatically and effortlessly. Existing approaches focus on only a few known pressure-perturbation thresholds (e.g., +1.0 and -1.0 hPa) and lack the ability to evaluate those parameter choices in an efficient manner. Exploring the full range of parameter values (i.e., pressure-perturbation thresholds) allows scientists to understand how an event's behavior and attributes change as the pressure-perturbation value varies, and thus, they are able to better characterize that event.

Second, when exploring the evolution of pressure-perturbation events, scientists also wish to compare an event's evolution with respect to different feature correlation metrics. Almost all existing atmospheric tools consider a single, distance-based correlation metric. However, depending on the temporal resolution of the source data and the feature mobility across time, feature evolution results for the same data set can differ drastically based on the correlation metric used.

Third, the evolution of pressure-perturbation events needs to be visualized in a concise manner. When data sets with high spatial and temporal resolutions become available, the description of feature evolution becomes large and complex as well. In such a setting, it is often difficult to grasp the evolution of certain features at first glance, let alone identify salient ones, with conventional visualization tools. Here, a concise representation not only presents a global view of the feature evolution but also supports interactive parameter selection, feature extraction, and simplifications.

Fourth, exploring the coupling between positive- and negative-pressure-perturbation events is also of importance to the atmospheric scientists. A positive-pressure-perturbation event is often either followed or preceded by a propagating negative-pressure-perturbation event. The spatial gradients produced by these couplets are often physically related to a region of enhanced surface winds, further adding to the importance of these events. Therefore, exploring these events simultaneously in space and time allows for further physical understanding of global atmospheric phenomena.

Finally, leveraging additional atmospheric, geographic, and spatial data sets adds detailed explanations of the atmospheric phenomena responsible for pressure-perturbations. For example, radar imagery, which is an indication of precipitation intensity, can provide further information on the physical causes of these pressure-perturbations. Other observational resources such as temperature, wind, and moisture can provide further details on explaining why the pressure-perturbations are present.

## 4 Application Solutions

We focus on addressing the aforementioned challenges by extracting and tracking pressure-perturbation events in both space and time. First, by making use of advance data structures such as merge/split trees [3] and meta-graphs [25], we enable interactive exploration of features and their evolution for the entire parameter range. Next, we use tracking graphs to present a global, concise view of feature evolution over time. These tracking graphs can be simplified based on various feature attributes and correlations encoded in the above data structures. Also, as tracking graphs can be dynamically generated, they have the flexibility to be created with different correlation metrics; and the feature tracks can be filtered at run-time based on various feature attributes. Finally, we allow simultaneous exploration of both positive- and negative-pressure-perturbation events by making concurrent adjustments to multiple pressure-perturbation thresholds.

In this work, we enhance and extend a prior system [25, 26] that relies on dynamically constructed tracking graphs to enable feature extraction, tracking, and simplification. Specifically, several new functionalities have been developed to fit the needs of atmospheric scientists, such as run-time filtering of feature tracks based on event characterizations; simultaneous exploration of multiple feature hierarchies and visualization of feature evolution over time; histogram views that summarize the stability of features within each time step; and geospatial views that display each feature's geographic location and trajectory information. Furthermore, to better understand the global atmospheric phenomena, we visualize pressure-perturbation events alongside other ancillary data sets such as radar imagery and wind observations. We now highlight our contributions.

From an atmospheric sciences point of view, our work not only improves existing analysis tasks, but also inspires several new ones:

- Exploring pressure-perturbation events within the full range of parameter values;
- Interactively visualizing the evolution of pressure-perturbation events using dynamically constructed tracking graphs;
- Extracting, filtering, and simplifying tracking graphs based on various attributes related to feature description, correlation, and characterization; and
- Leveraging additional atmospheric, geographic, and spatial data sets to further the understanding of global atmospheric phenomena.

From a visualization point of view, our work extends and enhances a prior system [25, 26] by adding new functionalities, including:

- Run-time computation of attributes related to event characterization and filtering of feature tracks;
- Simultaneous exploration of multiple feature hierarchies and visualization of feature evolution;
- Integration of histogram and geospatial-based visualizations geared toward atmospheric scientists; and
- Incorporation of ancillary data sets to enhance the data analysis process.

## 5 Atmospheric Sciences Data sets

In this work, we make use of the same data sets generated for the atmospheric research initiatives addressed in [10]. The atmospheric pressure observations used arise from a unique field campaign within the geosciences called the USArray Transportable Array (TA) [19, 27]. The TA, as part of the National Science Foundation sponsored EarthScope program, contained a set of pressure sensors separated by $\approx$80 km and deployed in a pseudo-grid fashion across a portion of the United States for a 1- to 2-yr period. Sensors were then retrieved and deployed further east, resulting in what appeared to be a "discrete eastward movement" of the array over time as shown in Figure 3. As a result, very high temporal resolution (1Hz observed)

surface pressure observations for a roughly 2-yr period are available from each location in the figure. However, the spatial resolution of the USArray TA data set is not adequate on its own to represent some of the mesoscale pressure-perturbations of interest.

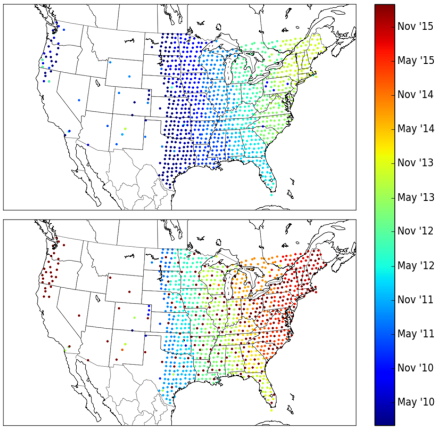


Figure 3: A set of seismic stations are deployed as a part of the National Science Foundation sponsored EarthScope USArray TA project [19, 27]. Here, the seismic station locations from January 1, 2010 to February 29, 2016 are displayed. For each station, the marker colors denote the first (top) and last (bottom) date of its pressure observations. Figure is adapted from [11].

For that reason, the data set we utilize here incorporates an additional resource. This resource contains information at a higher spatial resolution than the TA observations. Described further by [10], surface pressure grids produced by the National Centers for Environmental Prediction Real Time Mesoscale Analysis (RTMA) [20] were acquired with a horizontal spacing of 5 km. The acquired grids (TA observations) were interpolated (sub-sampled) to 5 min data intervals to align temporal frequency. Using the University of Utah Two-Dimensional Variational Analysis (UU2DVAR) technique [24], [10] blended the TA observations and RTMA grids together to produce a set of 5 km surface pressure analysis grids at 5 min intervals. These grids were then temporally band-pass filtered to isolate mesoscale pressure-perturbations of interest. The filtered gridded data set provided by [10], available for March 1 - August 31, 2011 over the central US, serves as the primary data set used in this work to identify and extract mesoscale pressure-perturbations.

In order to better identify and collocate pressure-perturbation events with atmospheric phenomena that might be causing them, additional data sets are required. Conventional radar reflectivity imagery is heavily used by atmospheric scientists to identify regions of precipitation often associated with thunderstorms and other high-impact weather systems. The Iowa Environmental Mesonet (IEM) provides an open-source web mapping service to leverage current and archived radar images, and is utilized as an additional data set in this work [8]. Additionally, surface wind observations can also be utilized to identify pressure-perturbation events with damaging winds. The wind observations for this work are acquired via MesoWest [9] for incorporation with the radar and pressure feature data sets through the utilization of MesoWest API services [1]. Here, wind observations from the standardized National Weather Service and Bureau of Land Management weather station networks are used to ensure stations with representative wind data.

## 6 System

We believe a system for visually exploring feature evolution should typically require three major capabilities: first, to construct a hierarchical representation of features within a time step; second, to correlate features over time; and third, to enable visual exploration of feature evolution across different scales spatially and temporally. In this work, we refine a prior system with the above capabilities that serves as an interactive exploration platform for dynamically constructed tracking graphs [25, 26]. This system is designed to study general time-varying features; however, so far it has been applied only to combustion data sets. We enhance and extend it to be successfully applied to atmospheric data sets. In doing so, we not only utilize existing functionalities but also introduce several new capabilities specifically tailored for the atmospheric scientists.

**Hierarchical Feature Representation and Correlation.** To store feature details, as in [25, 26], we enable a collection of standard clustering algorithms to be applied for obtaining hierarchical representations of features within a time step. Such a process encompasses feature segmentation and feature characterization. The precomputation of a hierarchical representation together with feature attributes allows quick feature extraction for any parameter value.

We also allow a collection of metrics to be applied during the feature correlation process (e.g., region overlap and distance proximity). Along with feature correlations details, various correlation-based attributes are also precomputed and stored, using the meta-graph structure [25, 26].

**Data Visualization.** Our visualization and analysis environment contains three views, see Figure 2: (a) feature embedding view, (b) feature hierarchy view, and (c) feature tracking view. The first presents a focused view for feature embeddings, whereas the last two present general conceptual views of the time-dependent features.

The feature embedding view uses two sub-views (geometric embedding and the geospatial) to present the data embedding of features within a focused time step, see Figure 2a. The geometric embedding sub-view displays features using a user-defined geometric embedding method (Figure 2a left), and the geospatial sub-view displays each feature's geographic location and trajectory information along with their radar imagery and wind observations (Figure 2a right). Combined, these sub-views enable scientists to explore regions of interest in both local and global contexts.

The feature hierarchy view visualizes the feature hierarchy within a focused time step, see Figure 2b. Here, a histogram-based sub-view that summarizes the stability of features for their entire parameter range is also included. Users have the flexibility to define the number of bins within the histogram. Figure 2b's histogram contains 56000 bins for the pressure-perturbation range $-2.8$ - $+2.8$ hPa. This histogram sub-view provides a quick overview of how the number of features changes as the threshold value is varied within a time step. Consequently, the feature hierarchy view enables scientists to understand the validity of the pressure-perturbation thresholds used within their analysis and also provides them the knowledge to vary the pressure-perturbation thresholds across time to obtain temporally cohesive tracking results.

Finally, within the feature tracking view, the evolution of features is visualized using tracking graphs, see Figure 2c. Starting from a focused time step, nodes and edges are iteratively added forward and backward in time up to a user-defined time window. For interactive exploration of tracking graphs, the same progressive graph layout techniques used in [25] are employed within this work. Specifically, a fast initial graph layout is used to quickly visualize the graph, and then the graph is updated using a slow greedy layout that uses a median heuristic to reduce the edge intersections. Within the tracking graph, nodes are colored by their size/volume, and for visual clarity the set of nodes in the focused time step is always displayed in prominent colors (for which a user-selected color map is used) whereas other nodes use a gray-scale color map. As shown in Figure 2c, users also have the option to scale the nodes based on their size/volume.

**Data Exploration.** Through a linked-view interface, users can explore data by changing the focused time step and time window. The parameters that define the feature hierarchies, correlations,

and attributes can all be explored via the tracking graph. As a result, tracking graphs can be filtered based on various attributes related to feature description and correlation. In the case of pressure-perturbation data, scientists are particularly interested in filtering tracking graphs based on attributes related to event characterization (e.g., total time of a feature existence, total distance a feature propagated, and maximum feature volume over its existence). So, our system also provides run-time computation of attributes related to event characterization and filtering of feature tracks. Specifically, for each feature track in the tracking graph, total time of existence, total propagation distance, and the average, standard deviation, median, maximum, and minimum of the following properties are computed over time: maximum/minimum magnitude value, long axis distance, short axis distance, eccentricity, area, propagation speed, and propagation direction.

Moreover, using the adaptive thresholding algorithm presented in [26], our system provides the capability to adaptively change feature threshold values over time to simplify tracking graphs. Specifically, for a tracking graph and a user-specified threshold range, feature thresholds within the graph are locally adapted to produce a more temporally cohesive graph.

Scientists are also interested in exploring both positive- and negative-pressure-perturbation events simultaneously in space and time. In this work, we allow changes to be made to two threshold values (i.e., positive- and negative-pressure-perturbation thresholds) simultaneously, thus enabling the extraction of feature and correlation details for both thresholds. This capability enables scientists to further explore the coupling structure within pressure-perturbation events and obtain a better understanding of global atmospheric phenomena.

## 7 Results

For the scope of this paper, we focus on three case studies from the data set provided by [10] for the March 1 - August 31, 2011 period. These case studies demonstrate the utility of visualizing short-term pressure-perturbations with respect to other conventional atmospheric science data sets such as radar imagery and surface wind observations to assess high-impact phenomena such as thunderstorms. The first two case studies contain discrete thunderstorm complexes and are used to demonstrate our system's ability to accurately assess pressure-perturbation events. The third case study provides a more complex meteorological situation and highlights the need for the flexible, interactive platform our system provides.

For each case study, an offline preprocessing step is used to compute the relevant feature hierarchies and their correlations. Here, scientists need to simultaneously explore both positive- and negative-pressure-perturbations events. They also wish to compare feature correlation results with respect to metrics based on spatial overlap and distance proximity. Therefore, for every time step in each case study, both merge tree and split tree structures are computed to enable simultaneous exploration of positive- and negative- pressure-perturbation events, respectively. During construction, various feature-based attributes such as centroid, area, median magnitude value, maximum/minimum magnitude value, position of the maximum/minimum magnitude value, long axis distance, short axis distance, long axis orientation, eccentricity, propagation distance, and propagation speed are also computed and stored within the feature hierarchies. Next, for exploring the feature evolution with respect to both correlation metrics, we compute the necessary correlation details for each metric and store them within separate meta-graph structures. Here, the correlation amount (i.e., the amount of spatial overlap or the length of Euclidean distance between features) is stored as a correlation-based attribute within each meta-graph. Since the relevant feature hierarchies and correlation details are precomputed in this manner, our system provides the flexibility to perform real-time feature extraction and rendering.

In each case study, by exploring tracking graph results, scientists are able to gain quick insights into their underlying structure. Furthermore, with the use of our system, scientists are able to obtain additional insights for each of these case studies. In the first case study, several insights into an appropriate pressure-perturbation threshold range for the event with a bow-like structure are obtained. For the second case study, tracking graphs for +1.0 hPa reveal an inconsistent evolution of one of its complexes. This insight inspired our scientists to use adaptive thresholds to allow for further detection of that event. Moreover, use of ancillary data sets within our system facilitated important insights into the coupling of positive- and negative- pressure-perturbation events within this second case study. For the final case study, exploration using our system reveals the existence of stationary noise within the data set. This insight inspired our collaborating scientists to improve their existing work flow to remove background noise more effectively, thus producing better preprocessed data sets.

### 7.1 Case Study I: Thunderstorm Complexes 08/2011

The first case study involves the development and movement of several distinct mesoscale thunderstorm complexes over the Great Plains. These events took place from 2100 Universal Coordinated Time (UTC) on August 11, 2011 through 0000 UTC on August 13, 2011. Several complexes produced wind damage, large hail, and tornado reports across South Dakota and northern Nebraska during the overnight period of August 11 (0000-1200 UTC August 12). Figure 4 displays radar imagery along with pressure-perturbations from the USArray TA stations courtesy of web products [2] developed as a part of research by the University of Utah Department of Atmospheric Sciences. Here, a bow-like structure is evident when viewing the weather radar imagery, leading to this type of convective complex being commonly referred to as a "bow echo". The markers denote the pressure-perturbation magnitudes recorded at several of the USArray TA stations, with red (blue) indicating positive- (negative-) pressure-perturbations.

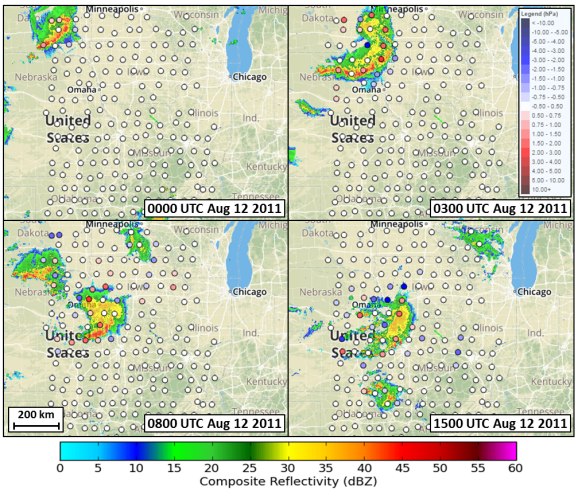


Figure 4: Case study I - Data : USArray mesoscale-filtered pressure-perturbations (hPa) are overlaid on composite radar reflectivity at 0000, 0300, 0800, and 1500 UTC August 12, 2011. Here, red circles indicate positive-pressure-perturbations and blue the negative-pressure-perturbations. The composite radar imagery is provided by the Iowa Environmental Mesonet web services.

The original data for this case study consists of 468 time steps and totals about 850MB. Once its feature hierarchies and correlation details are stored in our data format, the total data size is reduced to $\approx$70MB. It is important to note that a vast majority of this data is used for storing the list of feature and correlation-based attributes

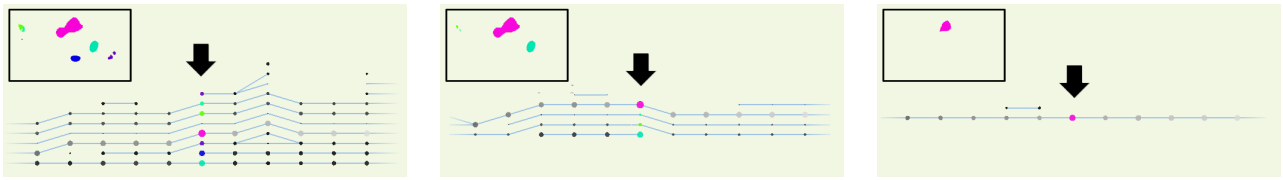

(a) +0.75 hPa (b) +1 hPa (c) +1.25 hPa

Figure 5: Case study I - Visualization : Effects of varying the pressure-perturbation threshold to explore the entire feature space. Here, pressure-perturbation events and a portion of their corresponding tracking graphs are shown at (a) +0.75 hPa, (b) +1.0 hPa, and (c) +1.25 hPa thresholds. In each case, the focused time step of the tracking graph is indicated with a black arrow.

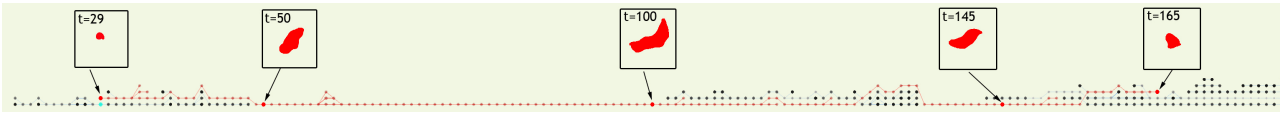


Figure 6: Case study I - Visualization : A longer tracking graph showing the evolution of pressure-perturbation events at +1.0 hPa. Here, the evolution of a feature with a bow-like structure is highlighted in red.

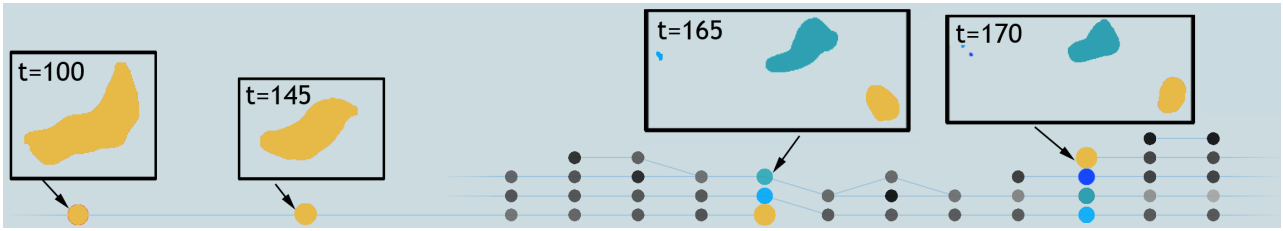


(a) Tracking graph at +1.0 hPa

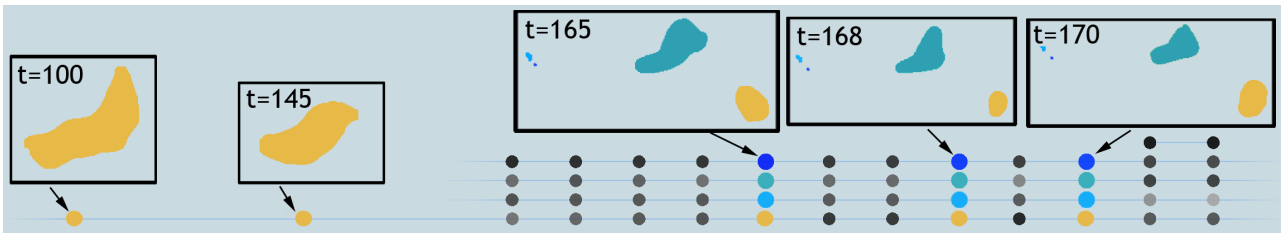


(b) Same tracking graph using adaptive thresholds

Figure 7: Case study I - Visualization : (a) A tracking graph at $+1.0$ hPa showing the sudden disappearance and reappearance of a feature with a bow-like structure (in yellow). Here, this feature disappears at $t = 165$ and then reappears at $t = 170$. Exploring the feature hierarchies reveals that this is likely due to variations in pressure-perturbation in-between time steps. (b) Therefore, by locally modifying the feature threshold values for those time steps (from $t = 165$ to $t = 170$), a much simpler graph where this feature is stably evolving can be obtained. In both cases, features at several time steps are visualized.

required for feature extraction and tracking, and spatial information needed for rendering. Here, we describe several key aspects of our framework that assist scientists explore and analyze this case study.

First, scientists are able to interactively explore the entire feature space by varying the pressure-perturbation threshold. Such exploration allows scientists to gain insights into which pressure-perturbation threshold range is reasonable for exploring a particular pressure-perturbation event. Figure 5 provides an example where pressure-perturbation events near the commonly used $+1.0$ hPa threshold are explored. Here, several positive-pressure-perturbation events in the spatial domain and a portion of their corresponding tracking graphs across pressure-perturbation thresholds of $+0.75$ hPa, $+1.0$ hPa, and $+1.25$ hPa are displayed. It is apparent that as the pressure-perturbation threshold increases, pressure-perturbation events decrease in both number and size (with only stable pressure-perturbation events remaining), and the resulting tracking graph reduces its complexity.

Second, the use of tracking graphs allows scientists to gain a global, concise view of the case study. They provide insights into the underlying structure of a particular pressure-perturbation event (its complexity, duration, and other trends). As shown in Figure 6, the resulting graphs indicate that several different weather systems existing within this case study and that they evolve (for the most part) distinctly over time.

Third, the adaptive thresholding component within our framework allows scientists to adaptively change the pressure-perturbation threshold over time to produce better, more consistent tracking results. For this case study, scientists are particularly interested in analyzing the evolution of the feature with a bow-like structure (yellow feature in Figure 7a). According to the tracking graph in Figure 7a, this feature exists for a long period of time, from $t = 100$ to $t = 145$ to $t = 165$, and disappears suddenly at $t = 165$ (i.e., $t = 100$ to $t = 165$ is 325 mins or 5.4 hrs). It then appears again at $t = 170$ and evolves from that point on. Further investigation reveals that this sudden disappearance and reappearance of the feature is due to variations in the pressure-perturbation between $t = 165$ and $t = 170$ and the chosen positive-pressure-perturbation threshold. Here, slightly reducing the pressure-perturbation threshold value for all time steps

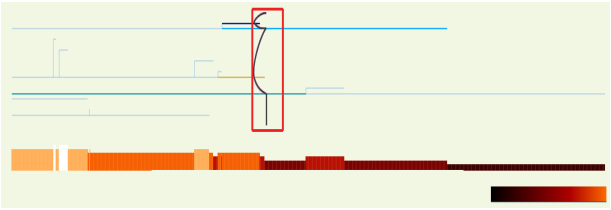

Figure 8: Case study I - Visualization : For the same tracking graph as in Figure 7b, the horizontal graph layout of the feature hierarchy (top) and the histogram sub-view (bottom) at $t = 168$, as shown within the feature hierarchy view. For this particular time step, the feature hierarchy is a forest with a pressure-perturbation range $+0.9$ - $+1.1$ hPa (increasing from left-to-right). Here, the histogram contains 3000 bins. The localized, per-feature thresholds are obtained by creating an arbitrary cut (indicated by the black vertical curve) within a user-defined threshold range (indicated by the red square).

$166 \leq t \leq 169$ (e.g., 0.88 hPa at $t = 168$) allows scientists to obtain a more temporally cohesive and easily comprehensible tracking graph, where this bow-like feature appears consistently across consecutive time steps between $165 \leq t \leq 170$, see Figure 7b. This adaptive thresholding component provides scientists insights into features-of-interest, in this case the bow-like structure. For a small pressure-perturbation threshold range around 1.0 hPa, this particular feature exists continuously for a longer period of time than at a fixed threshold value (i.e., 1.0 hPa).

Fourth, our framework's feature hierarchy view offers a detailed overview of the distribution and lifetime of features across multiple pressure-perturbation values within a given time step. Its histogram sub-view shows the number of pressure-perturbation events as a function of increasing the pressure-perturbation threshold, providing a quick overview of the feature variation across multiple pressure values, see Figure 8. The feature hierarchy view helps scientists choose an appropriate threshold range to obtain temporally cohesive tracking results. For the scenario described in Figure 7b, for one particular time step $t \in (165, 170)$, say, $t = 168$, an arbitrary cut (as indicated by the black vertical curve in Figure 8), for example, can be obtained within the feature hierarchy for a user-defined threshold range (as indicated by the red square in Figure 8). As a result of this arbitrary cut, in the final graph the number of features at $t = 168$ is more consistent with the number of features at $t = 165$ for threshold $+1$ hPa. This ability to define a reasonable threshold range by looking at the histogram sub-view helps generate more consistent tracking results.

### 7.2 Case Study II: Thunderstorm Complexes 06/2011

The second case study also provides a demonstration of our tool for discrete thunderstorm complexes. The first complex could be seen moving east across eastern Kansas into Missouri from 0300-0900 UTC June 18, while a second complex developed behind the first at 0600 UTC June 18 and moved east-northeast from 0600-1200 UTC June 18. Both thunderstorm complexes produced reports of wind damage, but the pressure-perturbations produced by these complexes varied in strength, highlighting the complexity of the physical processes associated with predicting and analyzing these events. The most pronounced pressure features were the negative-pressure-perturbation feature known as a "wake low" with the first complex, and the positive feature known as a "mesohigh" with the second complex [10]. The strength and proximity of these negative and positive features result in strong surface winds, which likely contributed to additional wind damage associated with the second complex. Figure 9 displays radar imagery along with the USArray TA pressure-perturbations for this case study.

The original data for this case study contains 192 time steps

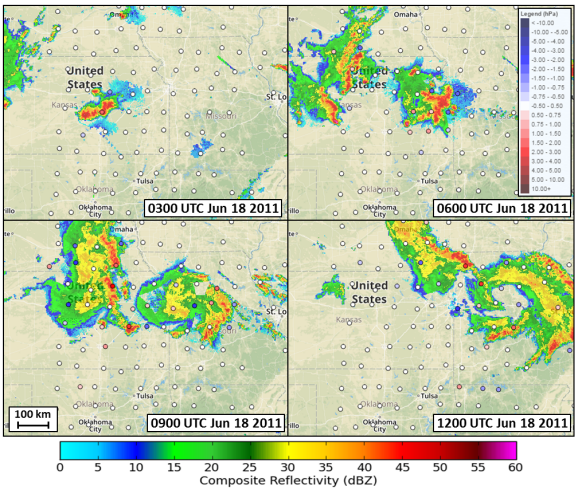


Figure 9: Case study II - Data : USArray mesoscale-filtered pressure-perturbations (hPa) are overlaid on composite radar reflectivity for 0300, 0600, 0900, and 1200 UTC June 18, 2011.

and totals ≈350MB of raw data. Once the feature hierarchies and correlation details are stored in our data format, the total data size is reduced to around 10MB. Several key aspects of our framework that assist in exploring this particular case study are described here.

First, scientists are able to explore the evolution of the pressure-perturbation events with the use of tracking graphs. As shown in Figure 10a, our system identifies the existing thunderstorms and visualizes their evolution over time.

As previously mentioned for the first case study, tracking graph results provide insights into the underlying structure of the pressure-perturbation event. For this case study, the tracking graph results indicate that the temporal evolution of one of the complexes (the one existing over eastern Kansas) is not very consistent across time. Further exploration reveals that this is due to the parameter choices and the complexity of this phenomenon. At the initial time steps, the thunderstorm complex is strong enough to be detected at the selected thresholds, but it loses its pressure magnitude over time. Here, the adaptive thresholding capability within our system is helpful in dynamically adapting the parameter choices within the tracking graph to allow for further detection of the pressure-perturbation event, see Figure 10b.

Next, our framework enables scientists to perform simultaneous exploration of multiple pressure-perturbation events across time. Such a capability enables scientists to simultaneously explore both positive- and negative- pressure-perturbation events and study their coupling structure, see Figure 11. In this case, the results provide insights into the strength of the coupling between the positive- and negative- pressure-perturbation events.

Finally, the ancillary information (i.e., radar and wind data) provided within our framework is particularly useful in gaining new insights into the atmospheric phenomena. For a specific time step, scientists can compare pressure-perturbation events (at varying thresholds) with the relevant radar imagery and also explore the relationships of these events with wind observations. Figure 12 shows an instance where the strong coupling of positive- and negative-pressure-perturbation events appears to be collocated well with very strong recorded wind speeds, which is to be expected physically due to the high pressure-perturbation gradients. Upon further exploration, these strong winds are not always perfectly collocated with radar observations, but rather they are located closer to the leading edge of the high-pressure-perturbation event. This insight is of significant interest to scientists as conventional meteorological tools are not be able to detect and assess such a phenomenon.

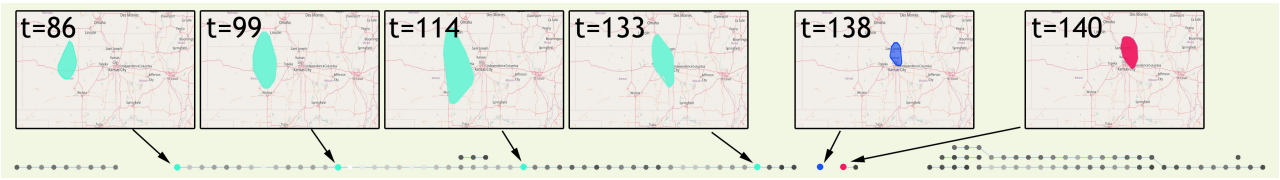


(a) Tracking graph for +1.0 hPa

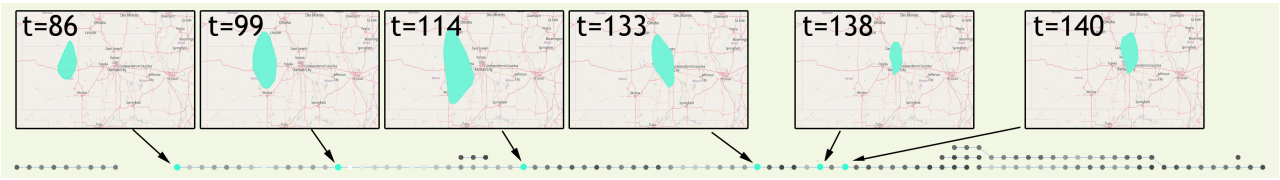


(b) Same tracking graph using adaptive thresholds

Figure 10: Case study II - Visualization : (a) A tracking graph showing the evolution of pressure-perturbation events for 113 time steps at +1.0 hPa. Here, one of the thunderstorm complexes (in green) is not consistent across time. This feature disappears at $t = 136$ and then reappears and dies at $t = 138$. Again, it reappears at $t = 140$ and later at $t = 146$. (b) The resulting tracking graph after adaptive feature thresholding is used to locally modify the features (in green) to allow continuous feature tracking.

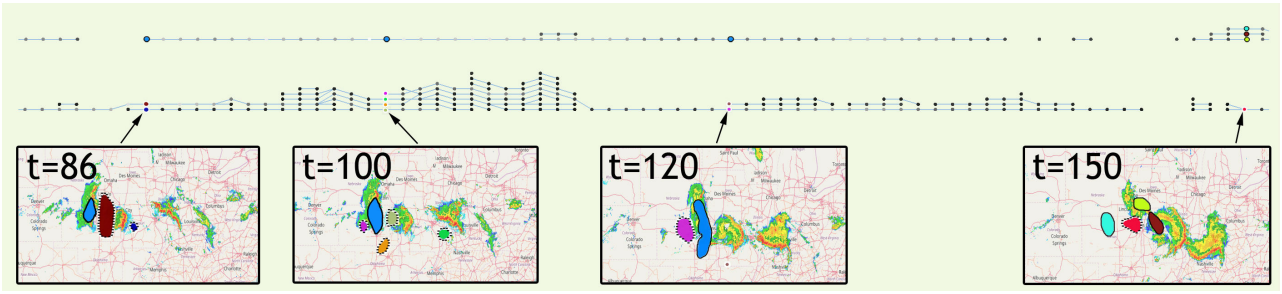


Figure 11: Case study II - Visualization : Simultaneously exploring both positive- and negative-pressure-perturbation events for multiple time steps. The graph on top shows the tracking graph at +1.0 hPa and the bottom at -1.0 hPa. Here, positive- (outlined in solid black line) and negative- (outlined in dashed black line) pressure-perturbation events existing at $t = 86, 100, 120$, and 150 time steps are also visualized.

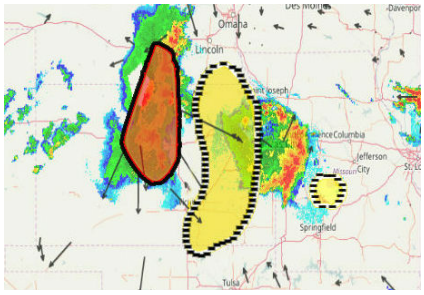


Figure 12: Case study II - Visualization : Both positive- (outlined in solid black line) and negative- (outlined in dashed black line) pressure-perturbation events are visualized alongside their radar imagery and wind observations (in black arrows). Here, the size and direction of winds are indicated by the arrow length and orientation. The image shows a strong coupling of positive- and negative-pressure-perturbation events. Such events are also collocated with strong winds going from the high- to low-pressure regions.

### 7.3 Case Study III: Severe Weather Outbreak 05/2011

The final case study demonstrates a very complex but fairly frequent meteorological situation. Severe weather and tornado outbreaks often occur when meteorological phenomena at various spatial and temporal scales interact with one another under the right atmospheric conditions. Due to these complex interactions, our tool provides a critical capability that allows the integration and variation of various data sets in real time. The case study described here took place from 0000 UTC May 24, 2011 to 0000 UTC May 26, 2011. The beginning of this period behaved similarly to the first case study with a discrete propagating mesoscale convective system moving southeast through Oklahoma and Arkansas. Another propagating system then formed and moved through northern Kansas from 1000-1700 UTC May 24. Beyond 2100 UTC May 24, a large-scale low-pressure system that formed over Eastern Colorado resulted in the development of several individual thunderstorms and mesoscale gravity waves. These individual thunderstorms then began to congeal into many linear segments as they propagated northeast from Oklahoma and Kansas and into Missouri. This event resulted in an extensive tornado and severe wind outbreak across Oklahoma and Kansas, with 11 deaths and over 290 injuries reported. Figure 13 displays radar imagery along with the USArray TA pressure-perturbations for this case study.

The original data contains 576 time steps and totals $\approx$ 670MB of raw data. Again, once its feature hierarchies and correlation details are stored in our data format, the total data size is reduced to around 400MB. Here, several key aspects of our framework assist in exploring this particular case study.

First, by exploring the feature evolution using tracking graphs, scientists are able to obtain a global overview of the weather system. The graphs reveal that this case study is more complex than the previous one, with large and complex graph structures, see Figure 14a.

Second, the ancillary data sets available within our system are able to provide additional information about the case study. As illustrated in Figure 15a, comparing features extracted from the pressure-perturbation data set against the radar imagery indicates the existence of noise. Our collaborating scientists found this insight

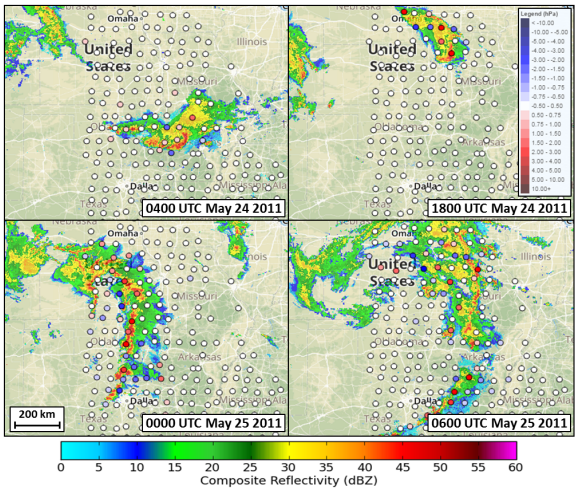


Figure 13: Case study III - Data : USArray mesoscale-filtered pressure-perturbations (hPa) are overlaid on composite radar reflectivity for 0400 UTC 24 May 2011, 1800 UTC 24 May 2011, 0000 UTC 25 May 2011, and 0600 UTC 25 May 2011.

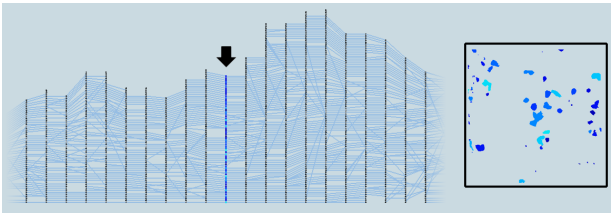

(a) Tracking graph for the original data set

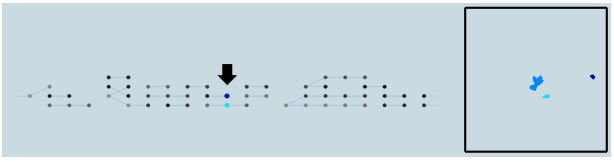

(b) Graph in (a) filtered by total propagation distance of a feature

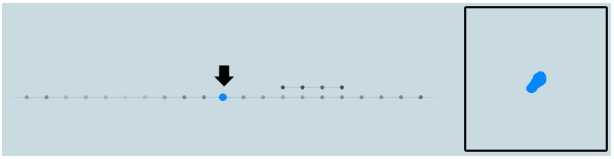

(c) Tracking graph for the cleaner, better preprocessed data set

Figure 14: Case study III - Visualization : (a) Tracking graph constructed from the original data set. (b) Tracking graph after filtering the graph in (a) by total propagation distance of a feature ($\geq$10). (c) For the same focused time window, its equivalent tracking graph for the better preprocessed data set. In each graph, the focused time step is indicated with a black arrow, and the features at the focused time step are visualized along each graph.

about the existence of noise is particularly useful as it provides means to validate their data sets.

Third, the ability to filter tracking graphs based on various feature- and correlation-based attributes enables scientists to separate true features from noise. Specifically, scientists are able to use *total propagation distance* of a feature to filter the tracking graphs and retain those features that are nonstationary, see Figure 14b. Those filtered, stationary features are considered to be background noise and are ignored in the analysis.

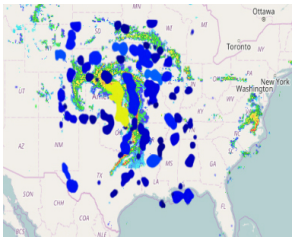

(a) Original data set

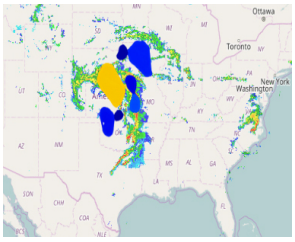

(b) Cleaner, better preprocessed data set

Figure 15: Case study III - Visualization : Features existing at +1.0 hPa for the same time step (at $t = 326$) in both (a) the original data set and (b) the cleaner, better preprocessed data set are visualized alongside their radar imagery. As indicated in the images, the preprocessed data set (b) contains less noise than the original data set (a).

This new insight regarding "stationary" noise within the data has inspired scientists to improve their preprocessing process, specifically the bandpass filtering step, to remove such background noise more effectively. Consequently, using their improved bandpass filter, a cleaner data set totaling $\approx$ 1.1GB is also generated for the same case study (Figure 15b). For this new data set, the total data size for the feature hierarchies and correlation details was around 80MB.

Figure 14c shows an equivalent but cleaner tracking graph of Figure 14a for this new data set. Again, for the new data set scientists are able to vary the pressure-perturbation threshold to explore the entire feature space and use tracking graphs to study the evolution of features. These tracking graphs highlight the complexity that takes place within this event, with several thunderstorm complexes merging, splitting, forming, and dissipating as shown in Figure 16.

## 8 Conclusion

In addition to the case studies presented here, several other case studies have also been analyzed using our framework and provided to atmospheric scientists for evaluation and feedback. According to the collaborating scientists, our system has been proven to be a powerful platform for conducting retrospective analysis to better understand different atmospheric phenomena. Specifically, the capability to explore features across multiple pressure-perturbation thresholds and the interactive abilities to thoroughly explore the tracking graphs are a distinct advantage over conventional techniques used in the field. As demonstrated by the three case studies, the visualizations provided by our interactive platform allow scientists to perform sensitivity analysis and to determine what pressure-perturbation thresholds appear valid for more accurate representations of the phenomena, as these thresholds are highly dependent on the concurrent atmospheric situation. Also, interactive assessment and filtering of feature properties, such as total feature area, feature lifetime, and feature movement (speed and direction), is also extremely useful for assessing which features are more prominent in the data sets of interest. Our collaborating scientists have indicated that our system could also have potential use for "nowcasting", which is short-term (0-6 hrs) forecasting of potential weather events. The system's interactive capabilities to extract, filter, and study certain pressure-perturbation events are appreciated in this kind of real-time setting. In terms of future improvements, we would like to use our system for short-term forecasting of certain weather events. We also aspire to include additional visual analytic tools such as [5, 18] within our system. A long-term goal is to leverage larger, more diverse data sets to broaden its use beyond identification and tracking of pressure-perturbation events.

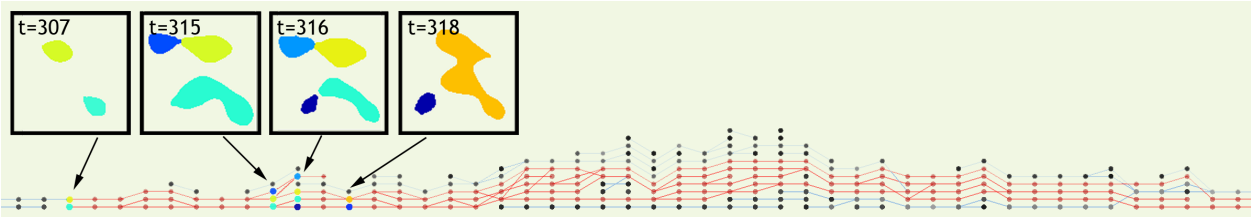


Figure 16: Case study III - Visualization : A longer tracking graph showing the evolution of pressure-perturbation events for 49 time steps at +1.0 hPa. For the two selected feature tracks in red, the features existing at $t = 307$, $t = 315$, $t = 316$, and $t = 318$ time steps are visualized. The graph clearly shows the complexity within this case study. Specifically, several thunderstorm complexes appear to merge, split, form, and dissipate.

## ACKNOWLEDGMENTS

This material is based upon work supported by the U.S. Department of Energy, Office of Science, Office of Advanced Scientific Computing Research, Scientific Discovery through Advanced Computing (SciDAC) program. This work was also performed under the auspices of the U.S. Department of Energy by Lawrence Livermore National Laboratory under Contract DE-AC52-07NA27344. This work also received funding support from the National Science Foundation Industry & University Cooperative Research Program (I/UCRC) # IIP-1439668. This research is partially supported by NSF-IIS-1513616. Funding for research involving the USArray pressure data was provided by National Science Foundation Grant ATM-1252315. USArray pressure data access was provided by the Incorporated Research Institutions of Seismology Web Services and the Array Network Facility at Scripps Institution of Oceanography, University of California San Diego. Storage of the USArray data was possible courtesy of the University of Utah Center for High Performance Computing (CHPC). Access to RTMA surface pressure grids and NARR reanalysis data were courtesy of web products available via the National Centers for Environmental Prediction.

## REFERENCES

[1] MesoWest & SynopticLabs APIs. `http://mesowest.org/api`. Accessed: 2016-09-26.

[2] Usarray microbarograph gui interface. `http://meso1.chpc.utah.edu/usarray/`. Accessed: 2016-09-26.

[3] P.-T. Bremer, G. Weber, V. Pascucci, M. Day, and J. Bell. Analyzing and tracking burning structures in lean premixed hydrogen flames. *IEEE Trans. Vis. Comp. Graph.*, 16(2):248–260, Mar. 2010. doi: 10.1109/TVCG.2009.69

[4] H. Carr, J. Snoeyink, and U. Axen. Computing contour trees in all dimensions. *Computational Geometry*, 24(2):75–94, 2003. doi: 10.1016/S0925-7721(02)00093-7

[5] M. Correll and M. Gleicher. The semantics of sketch: A visual query system for time series data. In *Proceedings of the 2016 IEEE Conference on Visual Analytics Science and Technology (VAST)*. IEEE, oct 2016. To appear.

[6] I. Fujishiro, Y. Maeda, and H. Sato. Interval volume: A solid fitting technique for volumetric data display and analysis. In *Proceedings of the 6th Conference on Visualization '95*, VIS '95, pp. 151–, 1995.

[7] A. Gyulassy, P.-T. Bremer, B. Hamann, and V. Pascucci. A practical approach to morse-smale complex computation: Scalability and generality. *IEEE Trans. Vis. Comp. Graph.*, 14(6):1619–1626, Nov. 2008. doi: 10.1109/TVCG.2008.110

[8] D. Herzmann, R. Arritt, and D. Todey. Iowa environmental mesonet. *Available at mesonet. agron. iastate. edu/request/coop/fe. phtml (verified 27 Sept. 2005). Iowa State Univ., Dep. of Agron., Ames, IA*, 2004.

[9] J. Horel, M. Splitt, L. Dunn, J. Pechmann, B. White, C. Ciliberti, S. Lazarus, J. Slemmer, D. Zaff, and J. Burks. Mesowest: Cooperative mesonets in the western united states. *Bulletin of the American Meteorological Society*, 83(2):211–225, 2002.

[10] A. Jacques. *Temporal and spatial analyses of pressure perturbations from the USArray Transportable Array*. PhD dissertation, Dept. of Atmospheric Sciences, University of Utah. In Press, 2016.

[11] A. A. Jacques, J. D. Horel, E. T. Crosman, and F. L. Vernon. Central and eastern us surface pressure variations derived from the usarray network. *Monthly Weather Review*, 143(4):1472–1493, 2015.

[12] D. S. Kalivas and A. A. Sawchuk. A region matching motion estimation algorithm. *CVGIP: Image Understanding*, 54(2):275–288, 1991.

[13] S. E. Koch and S. Saleeby. An automated system for the analysis of gravity waves and other mesoscale phenomena. *Weather and forecasting*, 16(6):661–679, 2001.

[14] W. E. Lorensen and H. E. Cline. Marching cubes: A high resolution 3d surface construction algorithm. *SIGGRAPH Comput. Graph.*, 21(4):163–169, Aug. 1987. doi: 10.1145/37402.37422

[15] C. F. Mass and L. E. Madaus. Surface pressure observations from smartphones: A potential revolution for high-resolution weather prediction? *Bulletin of the American Meteorological Society*, 95:1343–1349, 2014.

[16] N. D. Metz and L. F. Bosart. Derecho and mcs development, evolution, and multiscale interactions during 3-5 july 2003. *Monthly Weather Review*, 138(8):3048–3070, 2010.

[17] C. Muelder and K.-L. Ma. Rapid feature extraction and tracking through region morphing. Technical report, Citeseer, 2007.

[18] P. K. Muthumanickam, K. Vrotsou, M. Cooper, and J. Johansson. Shape grammar extraction for efficient query-by-sketch pattern matching in long time series. 2016.

[19] G. L. Pavlis, K. Sigloch, S. Burdick, M. J. Fouch, and F. L. Vernon. Unraveling the geometry of the farallon plate: Synthesis of three-dimensional imaging results from usarray. *Tectonophysics*, 532:82–102, 2012.

[20] M. S. F. V. D. Pondeca, G. S. Manikin, G. DiMego, S. G. Benjamin, D. F. Parrish, R. J. Purser, W.-S. Wu, J. D. Horel, D. T. Myrick, Y. Lin, R. M. Aune, D. Keyser, B. Colman, G. Mann, and J. Vavra. The real-time mesoscale analysis at noaa's national centers for environmental prediction: Current status and development. *Weather and Forecasting*, 26(5):593–612, 2011.

[21] M. K. Ramamurthy, R. M. Rauber, B. P. Collins, and N. K. Malhotra. A comparative study of large-amplitude gravity-wave events. *Monthly weather review*, 121(11):2951–2974, 1993.

[22] F. Reinders, F. H. Post, and H. J. W. Spoelder. Visualization of time-dependent data using feature tracking and event detection. *The Visual Computer*, 17:55–71, 2001.

[23] D. Silver and X. Wang. Tracking scalar features in unstructured data sets. In *Visualization'98. Proceedings*, pp. 79–86. IEEE, 1998.

[24] D. P. Tyndall and J. D. Horel. Impacts of mesonet observations on meteorological surface analyses. *Weather and Forecasting*, 28(1):254–269, 2013.

[25] W. Widanagamaachchi, C. Christensen, P.-T. Bremer, and V. Pascucci. Interactive exploration of large-scale time-varying data using dynamic tracking graphs. In *IEEE Symposium on Large Data Analysis and Visualization (LDAV), 2012*, pp. 9–17, 2012.

[26] W. Widanagamaachchi, P. Klacansky, H. Kolla, A. Bhagatwala, J. Chen, V. Pascucci, and P.-T. Bremer. Tracking features in embedded surfaces: Understanding extinction in turbulent combustion. *IEEE 5th Symposium on Large Data Analysis and Visualization*, pp. 9 – 16, 2015.

[27] Y. Yang and M. H. Ritzwoller. Teleseismic surface wave tomography in the western us using the transportable array component of usarray. *Geophysical Research Letters*, 35(4), 2008.